PS/Int. EA 60 - 4
4th April 1960

THE IDENTIFICATION OF HIGH ENERGY Λ^o's, $\overline{\Lambda^o}$'s AND θ^o's IN BUBBLE CHAMBER EXPERIMENTS

1. INTRODUCTION

In order to make efficient use of a large propane chamber in conjunction with beams from the PS, it is essential that the processes occurring in the chamber can be analysed with a good amount of certainty. In some high energy experiments involving strange particles one of the difficulties encountered is the identification of the decays:

$$\Lambda^o \rightarrow p + \pi^- + \sim 37 \text{ MeV},$$

$$\overline{\Lambda^o} \rightarrow \bar{p} + \pi^+ + \sim 37 \text{ MeV},$$

$$\theta^o \text{ (or } \overline{\theta^o}) \rightarrow \pi^+ + \pi^- + \sim 214 \text{ MeV},$$

due to the kinematic similarity of those decays at high energies. In this report we present a rough estimate of the probability of identifying a Λ^o, $\overline{\Lambda^o}$ or θ^o as a function of the momentum of the decaying particle, in the momentum range from 1 to 25 GeV/c.

Two general cases have been considered. In case I we have assumed that the total decay angle, the partial decay angles and the two secondary momenta are measurable, whereas in case II the above angles and only one secondary momentum are measurable.

To investigate these problems we considered three methods of analysis of neutral V-events:

a) the calculation of the Q - value;

b) the use of the α - p_t diagram;

c) the use of the α - ε diagram;

where α and ε are the well known parameters of Podolanski and Armenteros [1].

We have assumed that the identification of these particles is determined solely by the decay scheme and have ignored the possibility of further information from the production interaction or from interactions of the decay products, or from ionization measurements. Only identification of individual events was studied; for instance, the statistical distribution of the events in the $\alpha - \frac{1}{P}$ diagram which is often made was not considered.

To estimate the errors in the computed quantities involved, what seem reasonable errors in the measured quantities (momenta and angles) were assumed. Computer programmes have been used to calculate the kinematics and the associated errors. When experimentally determined measurement errors for a particular chamber are known it will be a relatively simple matter to replace our guesses at these quantities by the actual values.

In what follows an "identifiable Λ^o" means a V^o not compatible with the decay $\theta^o \rightarrow \pi^+ + \pi^-$. An "identifiable θ^o" means a V^o not compatible with the decays $\Lambda^o \rightarrow p + \pi^-$ and $\overline{\Lambda^o} \rightarrow \bar{p} + \pi^+$. Three-body decays have not been considered.

It was assumed that Λ^os, $\overline{\Lambda^o}$s and θ^os decay isotropically in their rest frame.

---

(1) : J. Podolanski and R. Armenteros: Phil. Mag. 45, 13 (1954).

2. NOMENCLATURE

Below is a list of the symbols used in this report and their meanings.

P = momentum of Λ^0 or θ^0 ;
p_+ = momentum of positive decay product ;
p_- = momentum of negative decay product ;
p_t = transverse component of momentum of either decay product ;
φ = angle in laboratory system between positive and negative decay products (decay angle) ;
φ_+ = angle in laboratory system between positive decay product and direction of primary particle ;
φ_- = angle in laboratory system between negative decay product and direction of primary particle ;
φ^* = angle in centre-of-mass system between positive decay product and direction of primary particle.

3. CASE I. IDENTIFICATION WHEN p_+, p_-, φ_+, φ_- AND φ ARE MEASURABLE

3.1 Identification by means of Q - values

For the case of a Λ^0 decaying to a proton and a π^-, for a given momentum P of the Λ^0 the angle φ^* was varied between 0° and 180°, and the two secondary momenta p_+ and p_- and the decay angle φ were calculated as a function of φ^*.

It was then assumed that these values of p_+, p_- and φ referred to a Θ^0, and the corresponding $Q(\pi, \pi)$ - values were calculated. To calculate the errors $\Delta Q(\pi, \pi)$ in these $Q(\pi, \pi)$ - values the following assumptions were made.

a) In a heavy liquid bubble chamber the main source of error in momentum measurement seems to be multiple scattering. This error can be calculated, and is found to lie roughly in the range 4 - 10% for particles of momentum greater than 1 GeV/c in most of the liquids currently used in large chambers, assuming a track length of about 50 cm and a magnetic field of 20 000 gauss. Consequently the assumption was made that the error in momentum is $\pm$ 10% and is independent of the value of the momentum.

b) The error in φ is $\pm$ 1° , which seems to be a realistic estimate.

c) The contributions of the errors in these three quantities are independent. *)

$$\Delta Q = \left[\left(\frac{\partial Q}{\partial p_+} \Delta p_+ \right)^2 + \left(\frac{\partial Q}{\partial p_-} \Delta p_- \right)^2 + \left(\frac{\partial Q}{\partial \varphi} \Delta \varphi \right)^2 \right]^{1/2} \qquad (1)$$

To be able to conclude that a Λ° is not mistaken for a Θ°, it is assumed that the $Q(\pi, \pi)$ - value as calculated above must be at least two standard deviations away from the Q - value of the Θ°, this latter incorporating the experimental error of one standard deviation.

*) The expressions for errors are given in full to indicate precisely which variables were used in their calculation.

Accordingly, for a given Λ^o momentum curves of $Q(\pi, \pi)$, $Q(\pi, \pi) + 2.\Delta Q(\pi, \pi)$ and $Q(\pi, \pi) - 2.\Delta Q(\pi, \pi)$ were plotted as a function of φ^*. On the same graph was plotted the Q - value of the Θ^o, taken as 214 ± 5 MeV. The region of overlap represents those Λ^o's which would not be distinguished from a Θ^o.

Since the curves are plotted as a function of φ^* the percentage of Λ^o's which are distinguishable is readily obtained.

This procedure was repeated for various Λ^o momenta, the diagrams for Λ^o's of 1, 5, and 10 GeV/c being shown in figures 1, 2 and 3 respectively. The resultant percentage of distinguishable Λ^o's is plotted as a function of the Λ^o momentum in curve A of figure 4.

To find the percentage of Θ^o's which are distinguishable from Λ^o's, the above procedure was applied to the Θ^o - decays. For a given momentum P of the Θ^o, φ^* was varied between 0^o and 180^o, and p_+, p_- and φ were calculated as a function of φ^*. The values of p_+, p_- and φ were used to calculate $Q(p, \pi)$ - values on the assumption that they referred to a Λ^o, and the above criteria were again applied. The diagram for Θ^o's of 5 GeV/c analysed as Λ^o's is shown in figure 5.

We assumed that if the $Q(p, \pi) + 2.\Delta Q(p, \pi)$ and $Q(p, \pi) - 2.\Delta Q(p, \pi)$ - values lie in the range 0 - 50 MeV the Θ^o was not distinguishable. We see from figure 5 that even if we extend this range to 0 - 100 MeV the percentage of identifiable Θ^o's is not greatly affected. The percentage of identifiable Θ^o's as a function of Θ^o momentum is shown in curve A of figure 6.

It is important to notice that the Q - value criterion gives the percentage of Θ^0's which are distinguishable from Λ^0's and from $\overline{\Lambda^0}$'s.

An important feature of the above analysis is the following. In deciding whether a Λ^0 of a given momentum was distinguishable from a Θ^0, no assumption was made about the momentum of the Θ^0. Consequently the figures obtained refer to the distinguishability of a Λ^0 of given momentum from a Θ^0 of <u>any</u> momentum, and similarly for the identification of a Θ^0.

3.2 Identification by means of the α - p_t diagram

Let us consider first the Λ^0's. As in the case of the Q - value criterion, for a given momentum P of the Λ^0 the angle φ^* was varied between 0^0 and 180^0, and p_+, p_-, φ_+, φ_- and φ were calculated as a function of φ^*. We then assumed that p_+ and p_- being both measurable, the parameter α is calculated from the expression:

$$\alpha = \frac{p_+^2 - p_-^2}{P^2} = \frac{p_+^2 - p_-^2}{p_+^2 + p_-^2 + 2p_+ p_- \cos\varphi} \qquad (2)$$

and that its error is then given by

$$\Delta\alpha = \left[\left(\frac{\partial\alpha}{\partial p_+}\Delta p_+\right)^2 + \left(\frac{\partial\alpha}{\partial p_-}\Delta p_-\right)^2 + \left(\frac{\partial\alpha}{\partial\varphi}\Delta\varphi\right)^2 \right]^{\frac{1}{2}} \qquad (3)$$

Due to the fact that in Λ^0 decay p_+ is greater than p_-, we used p_- and φ_- to calculate p_t in order to keep the errors as small as possible:

$$p_t = p_- \cdot \sin\varphi_- \qquad (4)$$

The curves of α plotted as a function of p_t are ellipses such as those shown in figures 7 and 8. The dots on the ellipses correspond to values of φ^* from 0° to 180° in steps of 10°.

To determine the error in α, it was assumed that as before the error in p_+ or p_- is constant and equal to 10% of the momentum. The errors in φ_+ and φ_- were optimistically taken to be $\pm 0.5^\circ$, and the error in φ to be $\pm 0.7^\circ$. Hence the standard deviations in α and p_t were calculated, and twice these values plotted on the α - p_t diagram for values of φ^* from 0° to 180° in steps of 10°. This is shown in figure 7 for the case of 5 GeV/c Λ°'s, the ellipse for the Θ°'s also corresponding to 5 GeV/c.

As in the case of the Q - value analysis, it was assumed that for a Λ° to be distinguishable from a Θ°, the point on the diagram corresponding to it must lie at least two standard deviations away from the Θ° curve. The range of values of φ^* for which this condition is satisfied gives us the percentage of identifiable Λ°'s of a given momentum. This percentage is plotted as a function of the Λ° momentum from 1 to 25 GeV/c in curve B of figure 4.

Referring to figure 7 it is seen that the error lines representing two standard deviations in the α's of the Λ° fall very close to the α - p_t curve of the Θ° for small C.M. angles φ^*, and it is largely a matter of taste whether the Λ°'s are considered distinguishable or not. The results represented by curve B of figure 4 were obtained by applying strictly the criterion described above, i.e. considering as identifiable all Λ°'s corresponding to small φ^* for which two standard deviations of α fall outside the α - p_t curve of the Θ°. The result of this is that the percentage of identifiable Λ°'s given by the α - p_t analysis (curve B of figure 4) is apparently appreciably higher

than the percentage of identifiable Λ^o's given by the Q - value analysis (curve A of figure 4). Now, in the Q - value analysis we included the uncertainty of 5 MeV in the accepted Q - value of the ϱ^o (214 $\pm$ 5 MeV). *) This same uncertainty can be included in the α - p_t analysis since the ϱ^o mass uncertainty will lead to an uncertainty in the value of α for the ϱ^o. If we take this into account, the Λ^o's corresponding to small values of φ^* will no longer be identifiable. In this case the number of identifiable Λ^o's given by the α - p_t criterion is the same as that given by the Q - value criterion, i.e. by curve A of figure 4.

Similar use of the α - p_t diagram was made to obtain the percentage of identifiable ϱ^o's of a given momentum. Figure 8 shows the plot of two standard deviations of α and of p_t for a ϱ^o of 5 GeV/c, for φ^* ranging from 0^o to 180^o in steps of 10^o. In the same figure the α - p_t curves for 5 GeV/c Λ^o's and $\overline{\Lambda^o}$'s are given.

The percentage of ϱ^o's that are distinguishable from Λ^o's and from $\overline{\Lambda^o}$'s as a function of the ϱ^o momentum, obtained from the α - p_t diagram, is again given by curve B of figure 6. If we ignore the $\overline{\Lambda^o}$'s, the percentage of ϱ^o's which are distinguishable from Λ^o's is given by curve B of figure 6, situated half-way between curve A and the line corresponding to 100%.

---

*) This takes into account the proposed shift of the Q - value of the ϱ^o to 219 MeV (A.H. Rosenfeld, F.T. Solmitz and R.D. Tripp: Phys. Rev. Lett., 2, 110 (1959)).

3.3 Identification by means of the $\alpha - \varepsilon$ diagram

In order to use the α and ε parameters, we constructed on the $\alpha - \varepsilon$ plane three families of curves corresponding to constant p_+, p_- and φ^* respectively, for the Λ^0 and the θ^0 decays. The curves relative to the θ^0 are shown in figure 9.

Let us consider first the identification of Λ^0's. For a given Λ^0 momentum, values of p_+, p_-, φ_+, φ_- and φ were calculated as a function of φ^*, as described in section 3.2. Then α and $\Delta\alpha$ have been calculated from expressions (2) and (3), and ε and $\Delta\varepsilon$ from:

$$\varepsilon = \frac{2p_t}{P} = \frac{2p_- \sin\varphi_-}{\left[p_+^2 + p_-^2 + 2p_+ p_- \cos\varphi\right]^{\frac{1}{2}}} \qquad (5)$$

$$\Delta\varepsilon = \left[\left(\frac{\partial\varepsilon}{\partial p_+}\Delta p_+\right)^2 + \left(\frac{\partial\varepsilon}{\partial p_-}\Delta p_-\right)^2 + \left(\frac{\partial\varepsilon}{\partial\varphi}\Delta\varphi\right)^2 + \left(\frac{\partial\varepsilon}{\partial\varphi_-}\Delta\varphi_-\right)^2\right]^{\frac{1}{2}} \qquad (6)$$

The errors in momenta and angles are the same as those assumed in section 3.2.

For each Λ^0 momentum we calculated a set of values of α, $\Delta\alpha$, ε, $\Delta\varepsilon$ corresponding to each value of φ^* from 0° to 180° in steps of 10°. The values of $\alpha \pm 2.\Delta\alpha$ and $\varepsilon \pm 2.\Delta\varepsilon$ corresponding to a Λ^0 of a given momentum were plotted on the $\alpha - \varepsilon$ plane of the θ^0 - decay. The ranges of values of p_+ and p_- covered by these errors were then read from the diagram. The Λ^0 was considered not identified if these ranges of values of p_+ and p_- covered the values corresponding to those of the π^+ and π^- emitted in the decay of a θ^0. The momentum of this θ^0 was taken to be equal to that of the Λ^0, but a spread was considered as the V^0 momentum cannot be determined precisely from the measured quantities.

Figure 9 shows the plot for Λ^0's of 1 GeV/c.

This procedure was repeated for various values of the Λ^0 momentum, so that a curve of probability of identification of a Λ^0 as a function of the Λ^0 momentum was obtained. This curve is practically the same as curve A of figure 4.

The identification of Θ^0's from the α and ε parameters was treated in a similar way. Values of $\alpha \pm 2.\Delta\alpha$ and $\varepsilon \pm 2.\Delta\varepsilon$ corresponding to a given momentum of Θ^0 were plotted on the $\alpha - \varepsilon$ plane of the Λ^0 decay. The resulting ranges of p_+ and p_- were compared with the values corresponding to a Λ^0, in the same way as described above. The probability of identification of a Θ^0 as a function of Θ^0 momentum, given by this criterion, is shown by curve D of figure 6. If the Θ^0's are to be identified from both Λ^0's and $\overline{\Lambda^0}$'s, curve C is obtained.

4. Case II. IDENTIFICATION WHEN φ_+, φ_-, φ AND ONE MOMENTUM ARE MEASURABLE

When only one secondary momentum can be measured well the resultant errors in the Q- value are so great that the Q - value becomes a less reliable criterion. Consequently only the $\alpha - p_t$ and $\alpha - \varepsilon$ analysis were considered in this case.

4.1 Identification by means of $\alpha - p_t$ diagram

As only one momentum is well measured, it was assumed that α and its errors are calculated from φ_+ and φ_- :

$$\alpha = \frac{\sin(\varphi_- - \varphi_+)}{\sin(\varphi_- + \varphi_+)} \qquad (7)$$

$$\Delta\alpha = \left[\left(\frac{\partial \alpha}{\partial \varphi_+} \Delta\varphi_+ \right)^2 + \left(\frac{\partial \alpha}{\partial \varphi_-} \Delta\varphi_- \right)^2 \right]^{\frac{1}{2}} \qquad (8)$$

Even with the optimistic assumption mentioned in section 3.2 that $\Delta\varphi_+$ and $\Delta\varphi_-$ are $\pm$ 0.5°, the errors in α are now much larger, by a factor between 2 and 5, than those obtained solely from errors in momentum.

The transverse momentum and its errors were calculated from p_- and φ_-.

By repeating the analysis described in 3.2 it is concluded that due to the large errors in α the number of identifiable Λ^0's is very much reduced. The α - p_t diagram for a Λ^0 of 5 GeV/c is given in figure 10. The percentage of Λ^0's which would be identifiable is shown in curve C of figure 4, as a function of the Λ^0 momentum. The percentage of identifiable Λ^0's in this case is much smaller than in case I.

An example of a similar analysis for Θ^0's is given in figure 11 for a Θ^0 of 5 GeV/c. The percentage of identifiable Θ^0's as a function of the Θ^0 momentum is again given by curve A or B of figure 6, depending on whether the $\overline{\Lambda^0}$'s are or are not included in the analysis. The result is that the percentage of identifiable Θ^0's of a given momentum is in this case the same as that obtained in case I.

4.2 Identification be means of the α - ε diagram

In case II it was assumed that α and $\Delta\alpha$ are given by expressions (7) and (8) respectively, and ε and $\Delta\varepsilon$ by:

$$\varepsilon = \frac{2 \sin\varphi_- \sin\varphi_+}{\sin(\varphi_- + \varphi_+)} \qquad (9)$$

$$\Delta\varepsilon = \left[\left(\frac{\partial\varepsilon}{\partial\varphi_+}\Delta\varphi_+\right)^2 + \left(\frac{\partial\varepsilon}{\partial\varphi_-}\Delta\varphi_-\right)^2\right]^{\frac{1}{2}} \qquad (10)$$

Even with $\Delta\varphi_+ = \Delta\varphi_- = \pm 0.5^\circ$ the errors in ε are much larger than those given by expression (6). The curves of constant p_+ and p_- on the $\alpha - \varepsilon$ plane were used as described in section 3.3. The result for Λ°'s is again given by curve C of figure 4. In the case of θ°'s the result is worse than is shown in figure 6, curves C and D, and was not plotted.

5. IDENTIFICATION OF ANTI - Λ°'s

As a consequence of the symmetry in the decays of the Λ° and $\overline{\Lambda^\circ}$, the results given in figure 4 are valid also for the $\overline{\Lambda^\circ}$.

6. CONCLUSIONS

It is worth repeating that we assumed that the only information available is that from the decay scheme itself, except for the point of production of the V° in the case when φ_+ and φ_- need to be determined. We did not consider a statistical distribution of events.

It is also worth emphasizing that, apart from the criteria adopted, the results expressed in figures 4 and 6 must be taken as approximate, and should not be trusted to better than 5%.

Under the assumption that the secondary momenta are measured with 10% error and the partial angles to $\pm 0.5^\circ$, the following first two conclusions are reached.

1) When φ_+, φ_-, φ and <u>both</u> secondary momenta are measurable, the percentage of identifiable Λ^o's as a function of Λ^o momentum is given by curve A of figure 4, whichever of the three methods of analysis is used. The percentage of identifiable Θ^o's as a function of Θ^o momentum is given in figure 6, as explained in the legend.

2) When φ_+, φ_-, φ and <u>one</u> secondary momentum are measurable, the percentage of identifiable Λ^o's is given by curve C of figure 4. Λ^o's with momentum greater than about 3 GeV/c will not be identified. The percentage of identifiable Θ^o's will be the same as in case I, provided one uses the α - p_t diagram.

The reason why the α - p_t diagram gives the same result for the Θ^o's in cases I and II, and gives a much worse result for Λ^o's in case II than in case I is the following. The identification of a Θ^o by means of this diagram depends strongly on p_t, which was made to have the same errors in both cases, while the identification of a Λ^o depends on α, which has larger errors in case II than in case I.

3) In many cases in practice it will not be possible to measure all the quantities used in case I (e.g. the decay may occur near the edge of the chamber, the tracks of the secondaries may be shorter than the 50 cm mentioned in section 3.1, the accuracy may not be uniform through the whole chamber, etc.). Since the probability of identification of a Λ^o found in case II is so very much worse than that of case I, it seems that the realistic probability of identification of Λ^o's will be appreciably less than that given by curve A of figure 4. On the other hand when the point of production of a Θ^o is known (which will generally be the case in a bubble chamber), the probability of identifying the Θ^o decay will never be much smaller than that given by curves A and B of figure 6.

4) The percentage of identifiable $\overline{\Lambda}^{o}$'s as a function of the $\overline{\Lambda}^{o}$ momentum will be the same as that for the Λ^{o} in cases I and II.

Finally, if the errors are different from those we assumed, the results can easily be changed by substituting in expressions (1), (3), (6), (8) and (10), the new errors assumed.

We should like to thank Drs. R. Armenteros, B.P. Gregory and A. Lagarrigue for profitable discussions.

R.A. Salmeron.
R.G.P. Voss.

Distribution : Magnet Group
(open) Parameter Committee

PS/1393

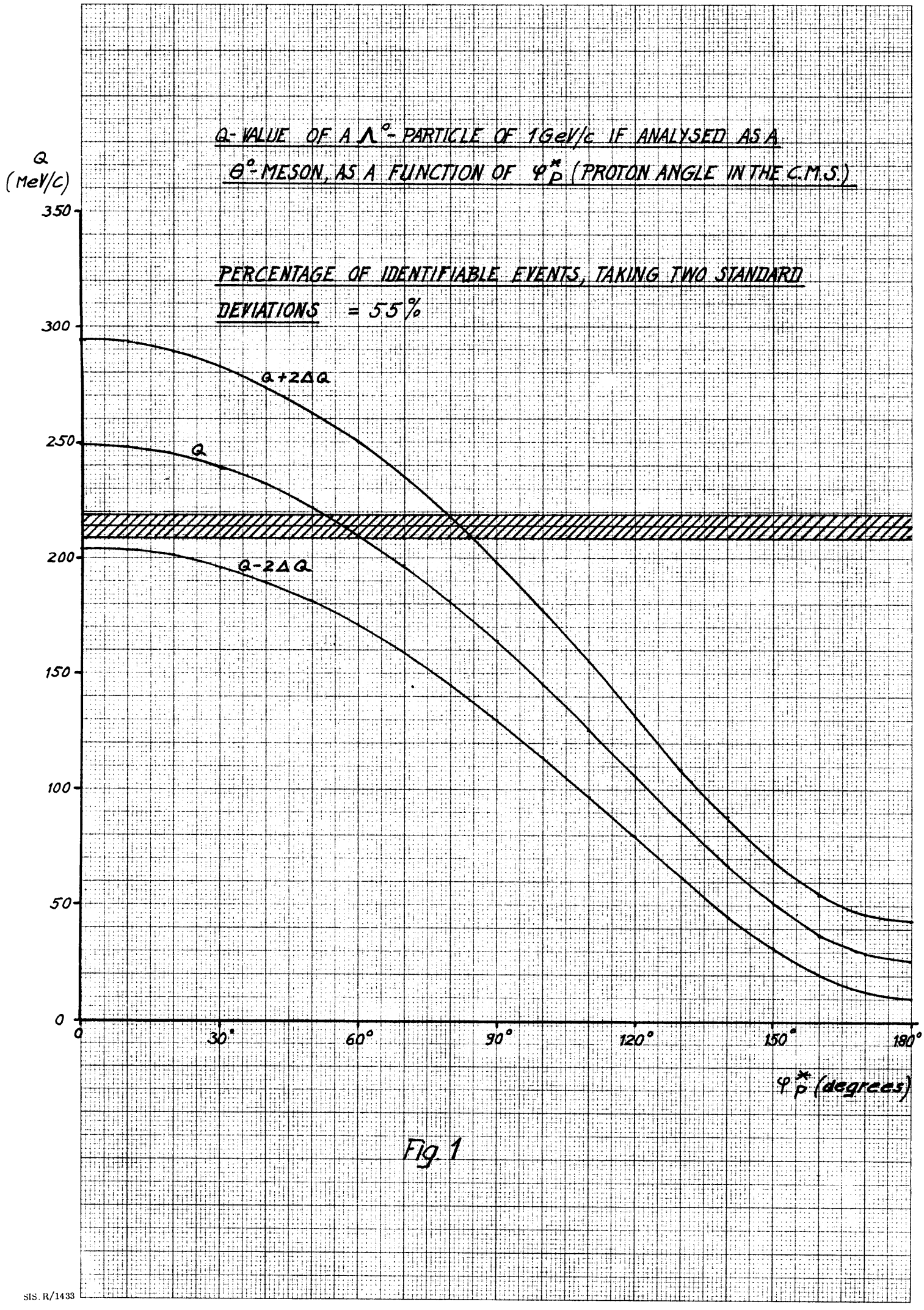

Fig. 1

SIS. R/1433

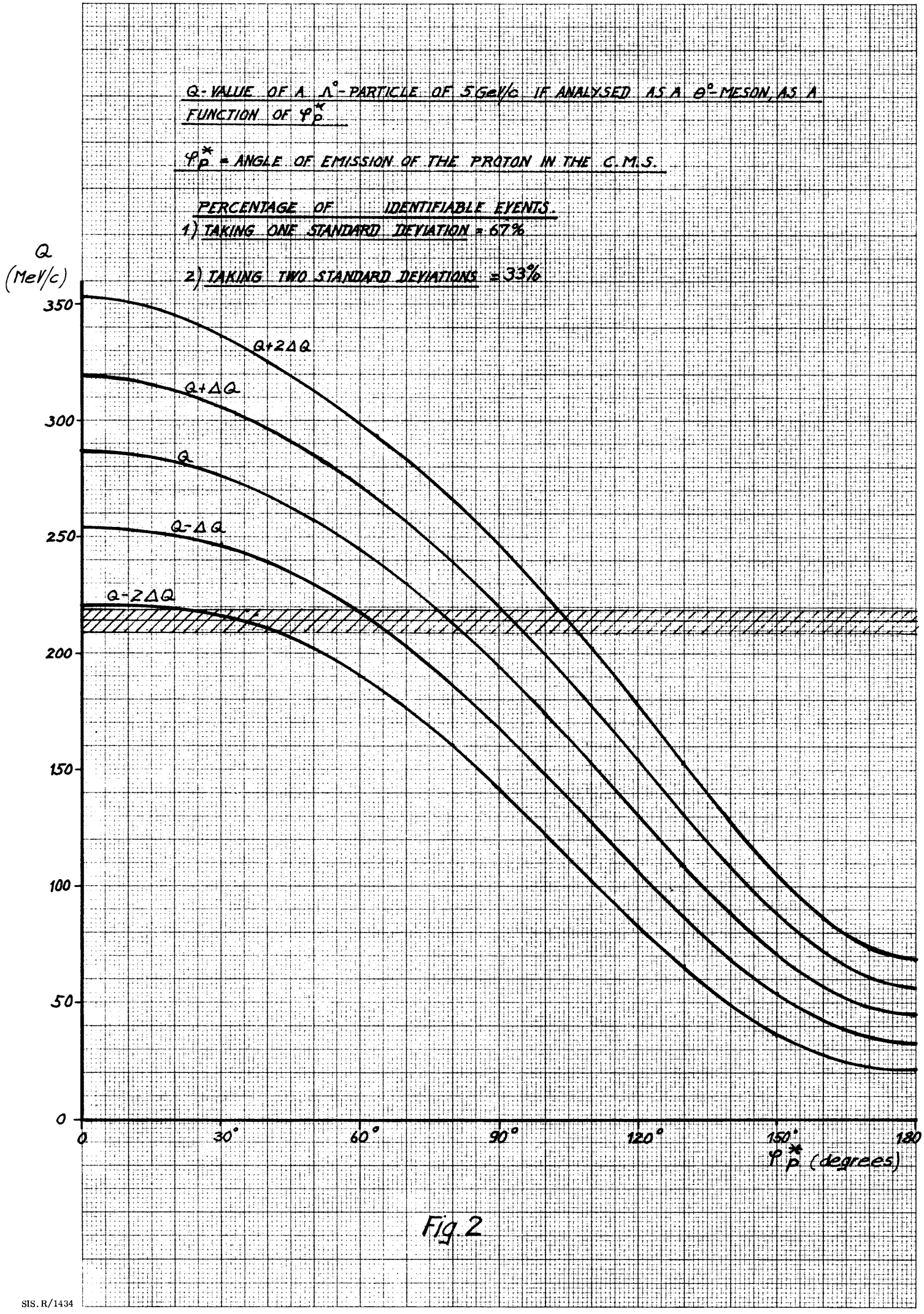

Fig. 2

SIS. R/1434

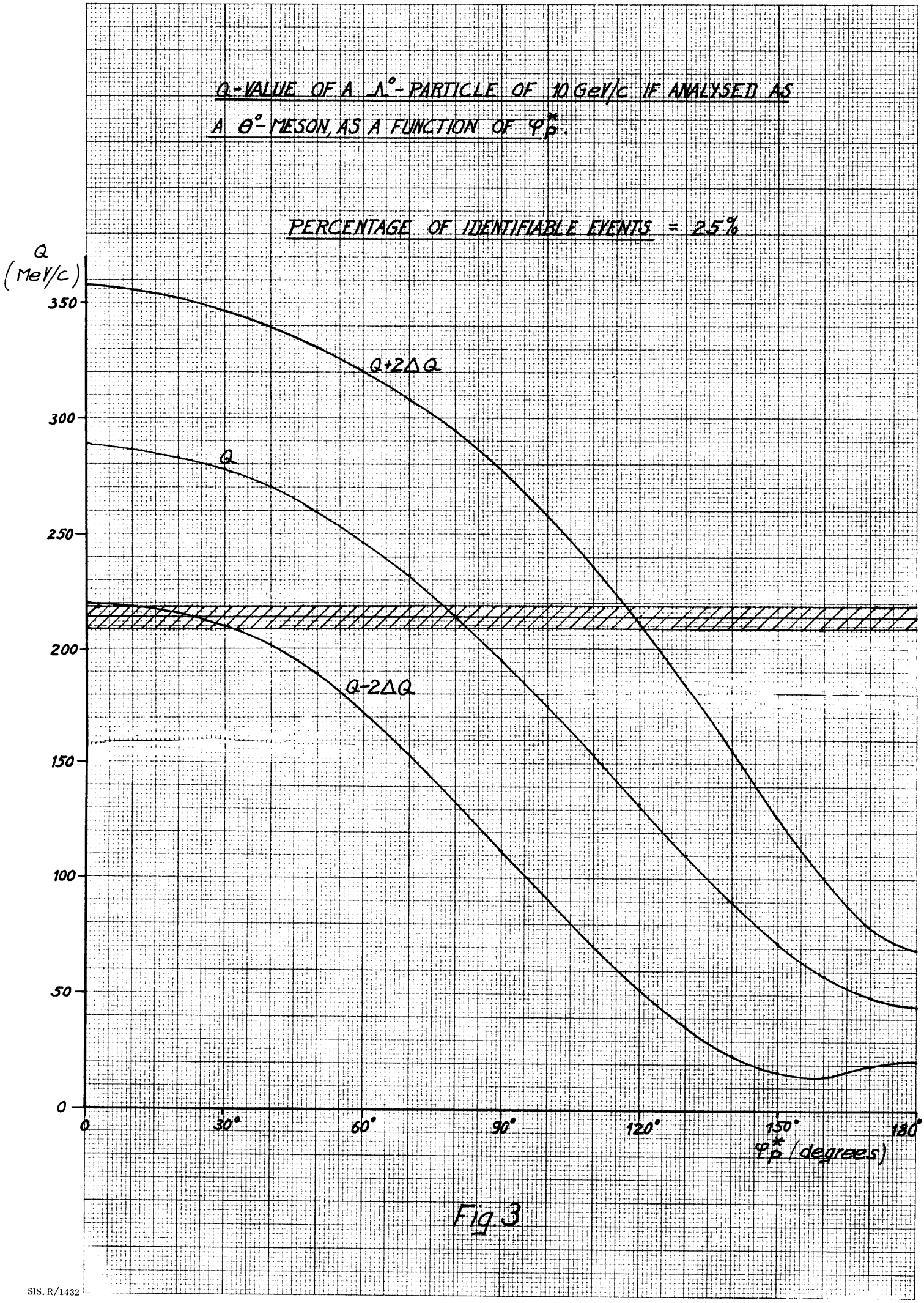
Q-VALUE OF A Λ°-PARTICLE OF 10 GeV/c IF ANALYSED AS A θ°-MESON, AS A FUNCTION OF φ*p.
PERCENTAGE OF IDENTIFIABLE EVENTS = 25%
Q (MeV/c)
350
300
250
200
150
100
50
0
Q+2ΔQ
Q
Q-2ΔQ
0
30°
60°
90°
120°
150°
180°
φ*p (degrees)

Fig. 3

SIS. R/1436

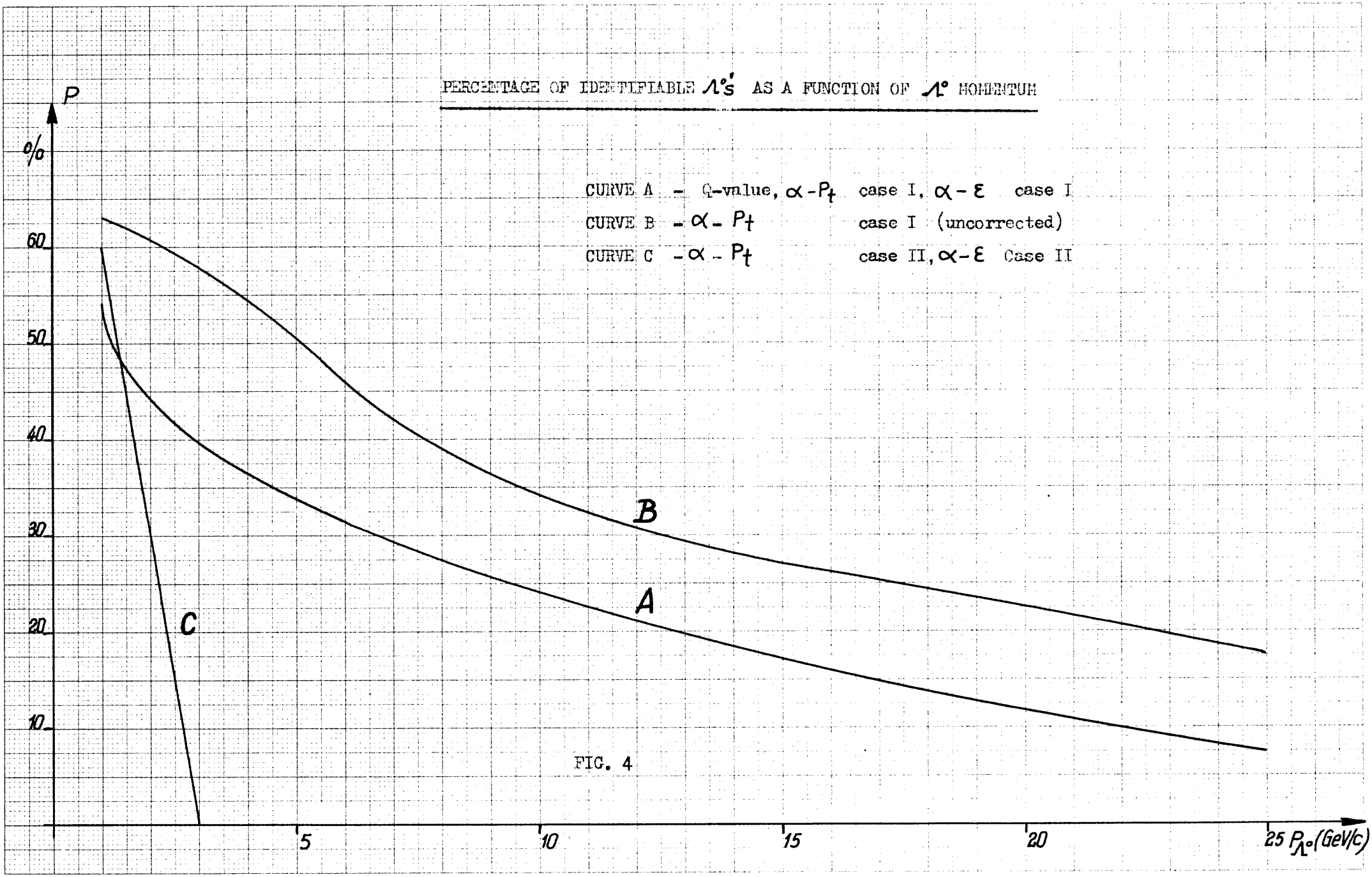

FIG. 4

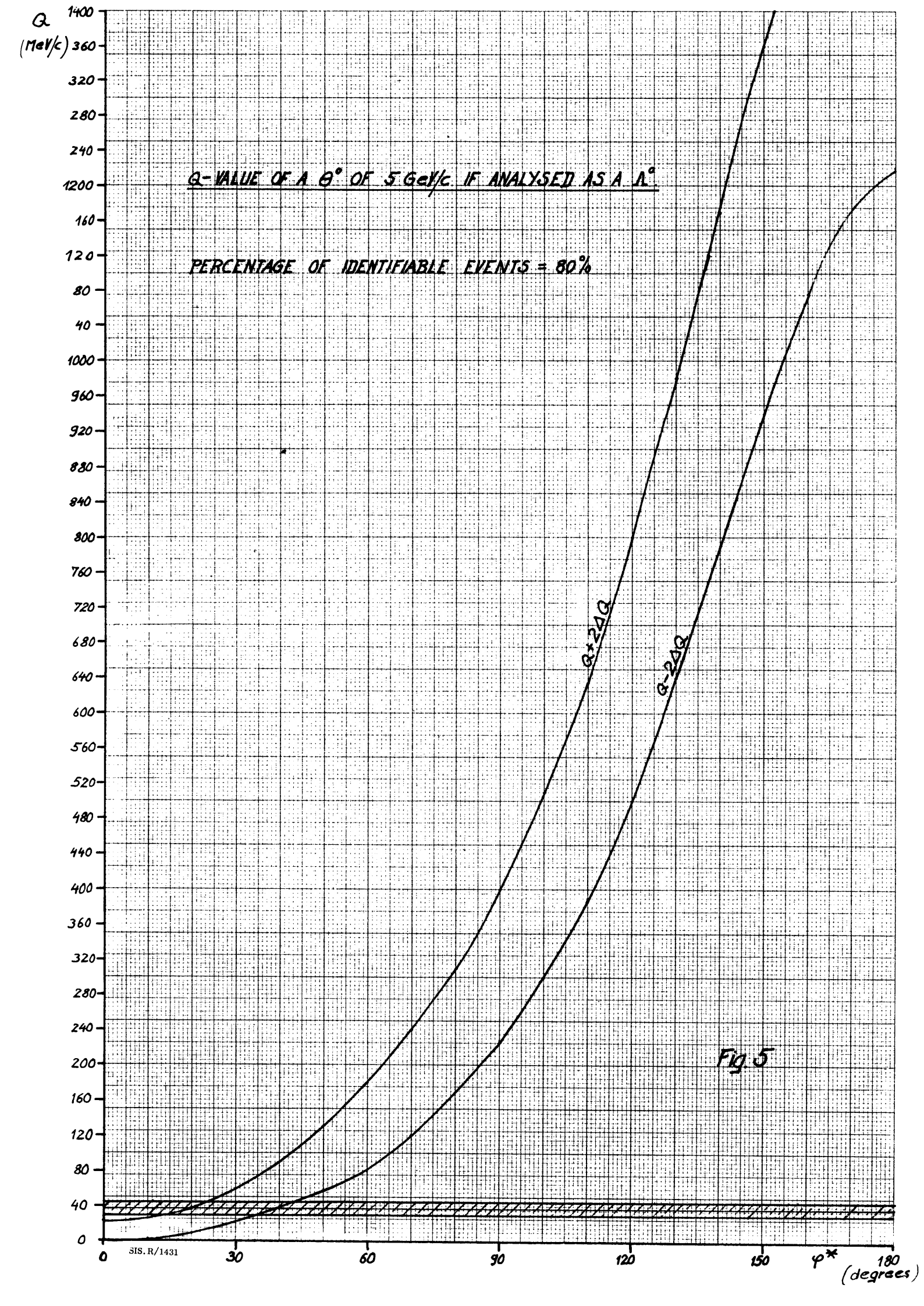
Q
(MeV/c)
Q-VALUE OF A Θ° OF 5 GeV/c IF ANALYSED AS A Λ°
PERCENTAGE OF IDENTIFIABLE EVENTS = 80%
Q+2ΔQ
Q-2ΔQ
φ*
(degrees)
SIS. R/1431

Fig. 5

SIS.R/1435

PERCENTAGE OF IDENTIFIABLE Θ°'s AS A FUNCTION OF Θ°- MOMENTUM

CURVE A - Q-value, $\alpha - P_t$ cases I and II ($\bar{\Lambda}^{\circ}$ included in the analysis)

CURVE B - $\alpha - P_t$ cases I and II ($\bar{\Lambda}^{\circ}$ not included in the analysis)

CURVE C - $\alpha - \varepsilon$ case I ($\bar{\Lambda}^{\circ}$ included in the analysis)

CURVE D - $\alpha - \varepsilon$ case I ($\bar{\Lambda}^{\circ}$ not included in the analysis)

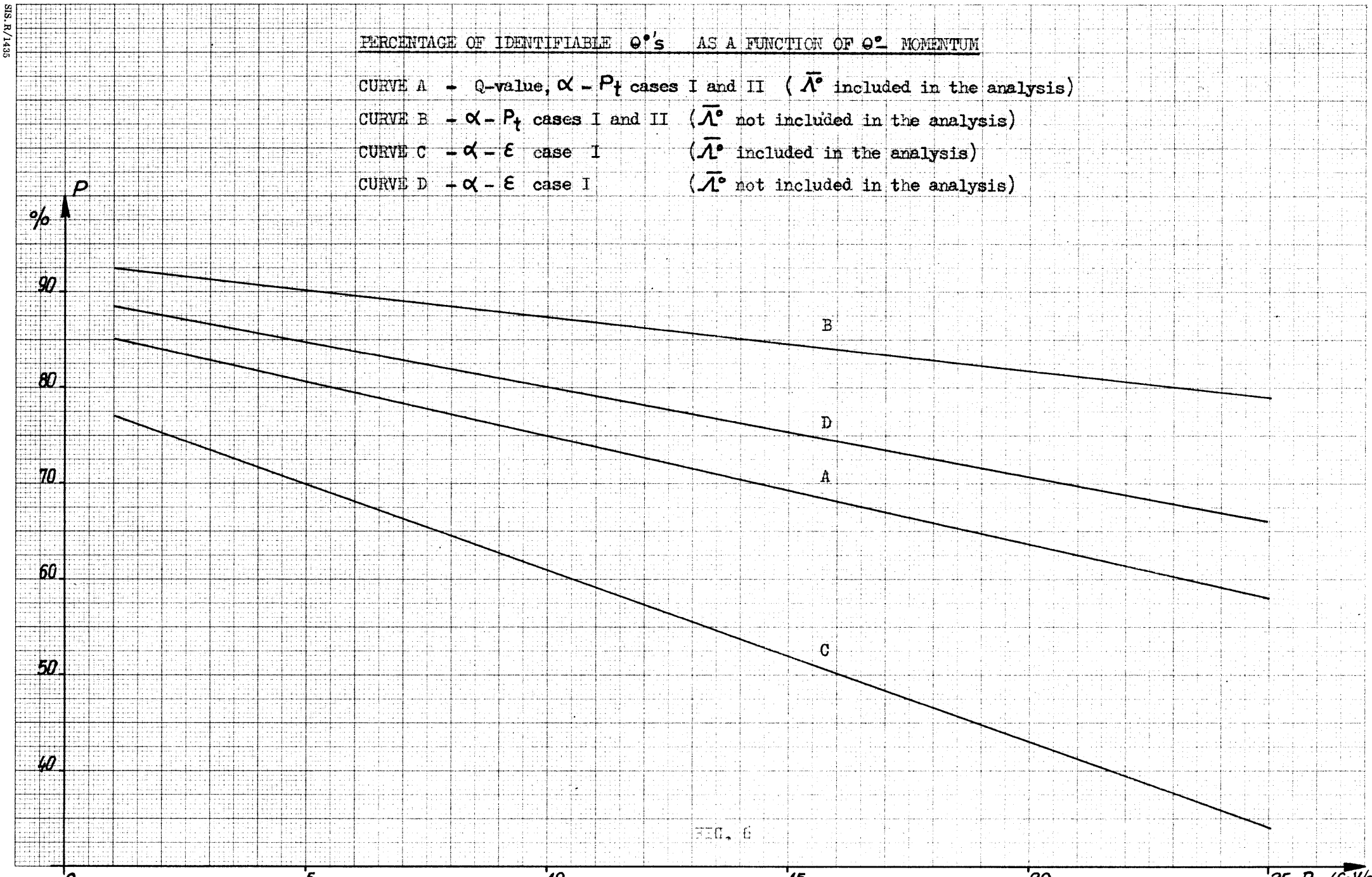

FIG. 6

$\alpha - P_t$ Diagram for Λ°, $\bar{\Lambda}^\circ$ and θ° of 5 GeV/c

Values of φ^* refer to positive secondary

Crosses show $\pm 2\Delta\alpha$ and $\pm 2\Delta P_t$ for a Λ° of 5 GeV/c in case I

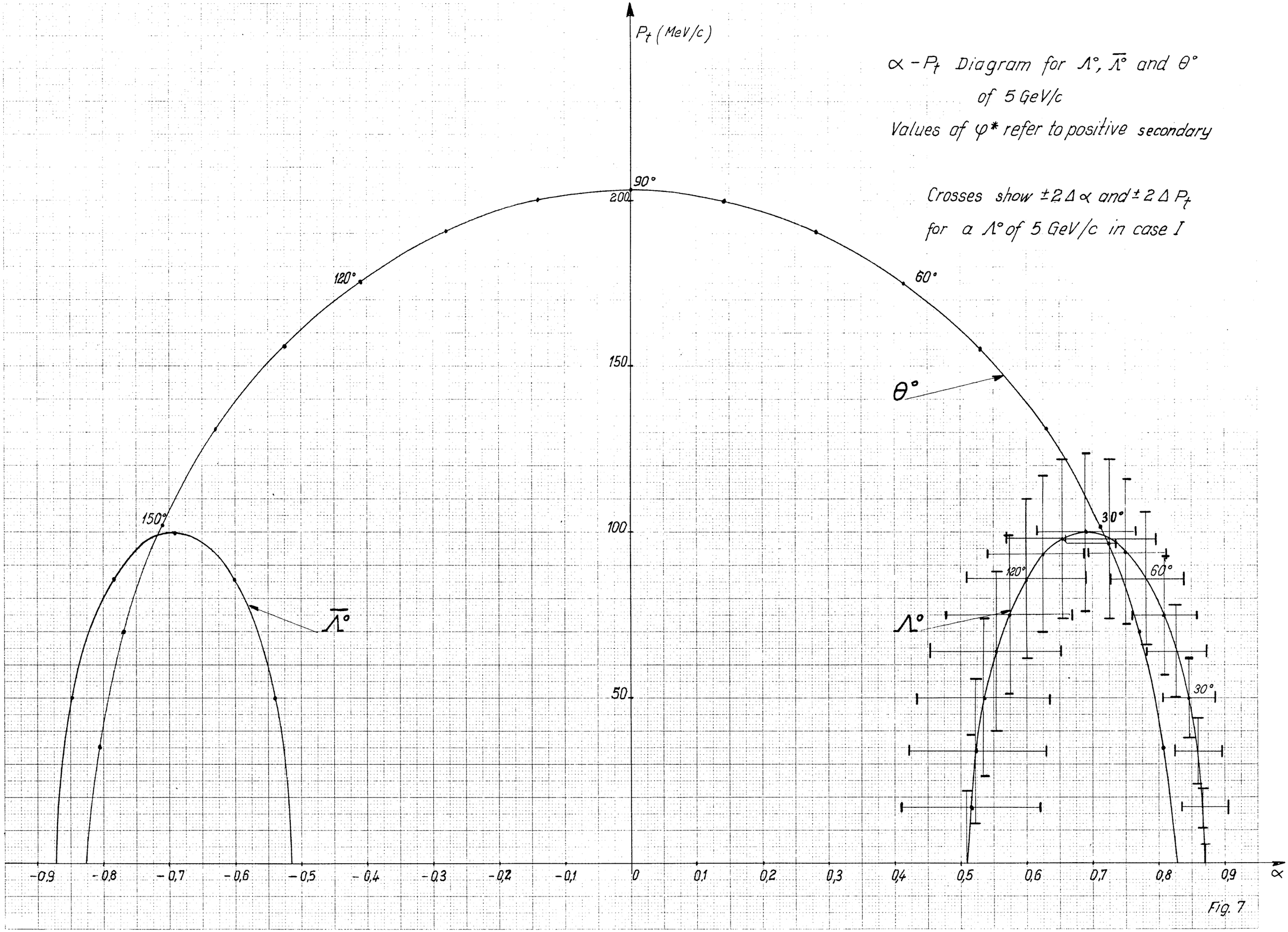

Fig. 7

$\alpha - P_t$ DIAGRAM FOR Λ°, $\bar{\Lambda}^\circ$ and θ of 5 GeV/c

values of φ^* refer to positive secondory

Crosses show $\pm 2\Delta\alpha$ and $\pm 2\Delta P_t$

for a θ° of 5 GeV/c in case I

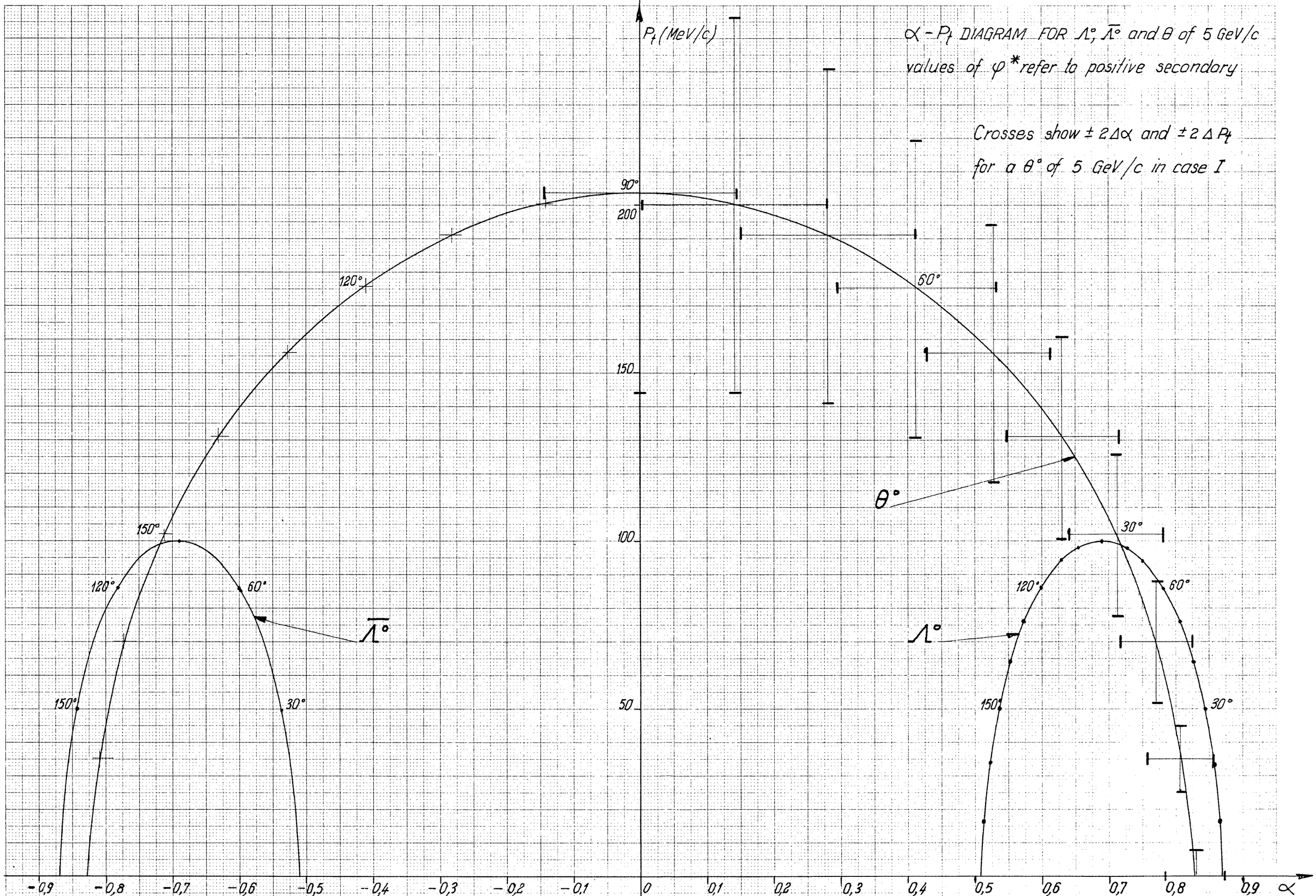

Fig. 8

Curves of constant p_+, p_- and φ_+^* for $\Theta°$

plotted on the $\alpha - \varepsilon$ diagram

The lines are the diagonals of the rectangles relative to the plat of $\alpha \pm 2.\Delta\alpha$ and $\varepsilon \pm 2.\Delta\varepsilon$ for a $\Lambda°$ of 1 GeV/c,
for φ_p^* of the proton from 0° to 180° in steps of 10°

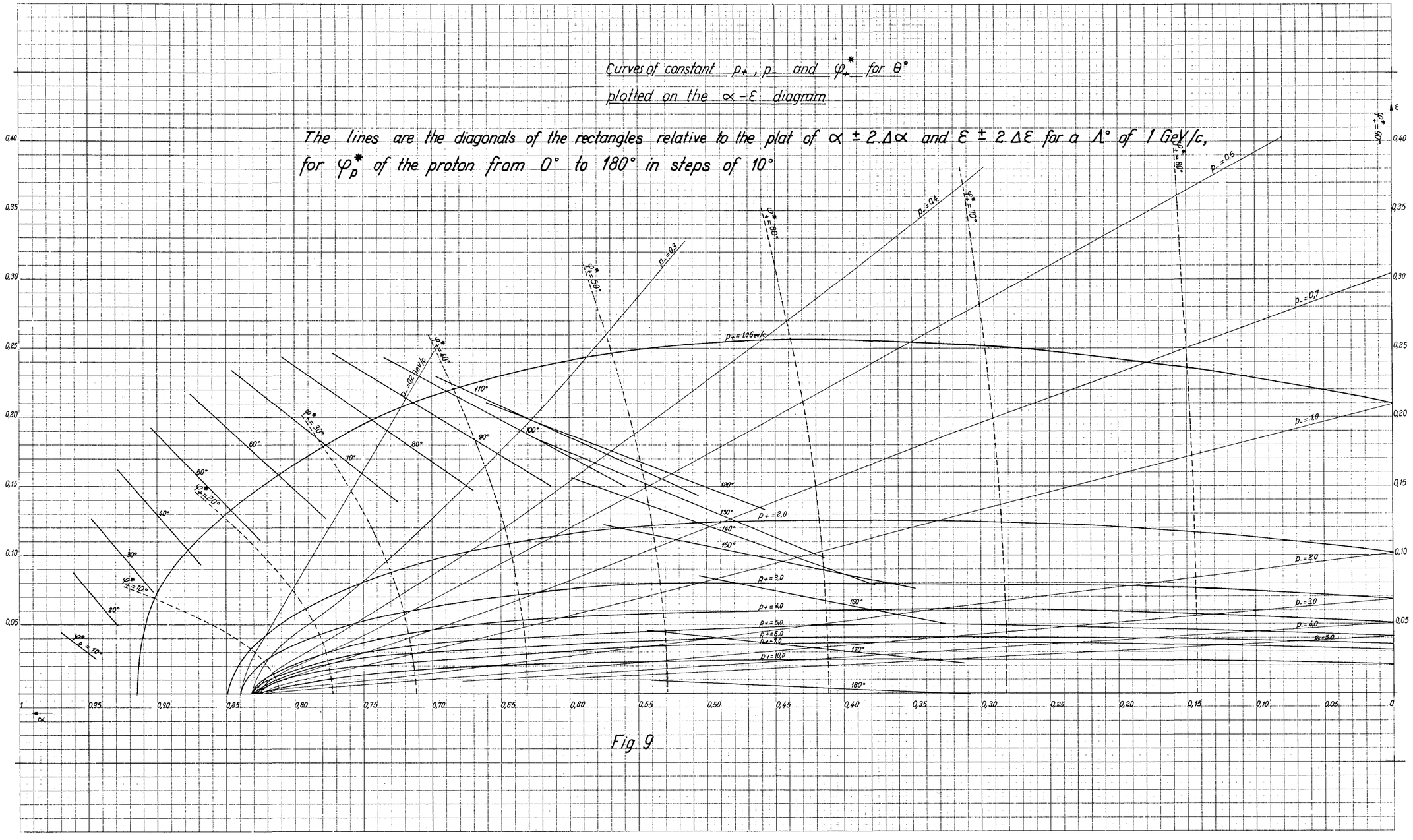

Fig. 9

α - P_t DIAGRAM FOR 5 GeV/c Λ°, $\bar{\Lambda}^\circ$ and θ°

Values of φ^* refer to positive secondary

Crosses show $\pm 2\,\Delta\alpha$ and $\pm 2\,\Delta p_t$ for a Λ° of 5 GeV/c in case II

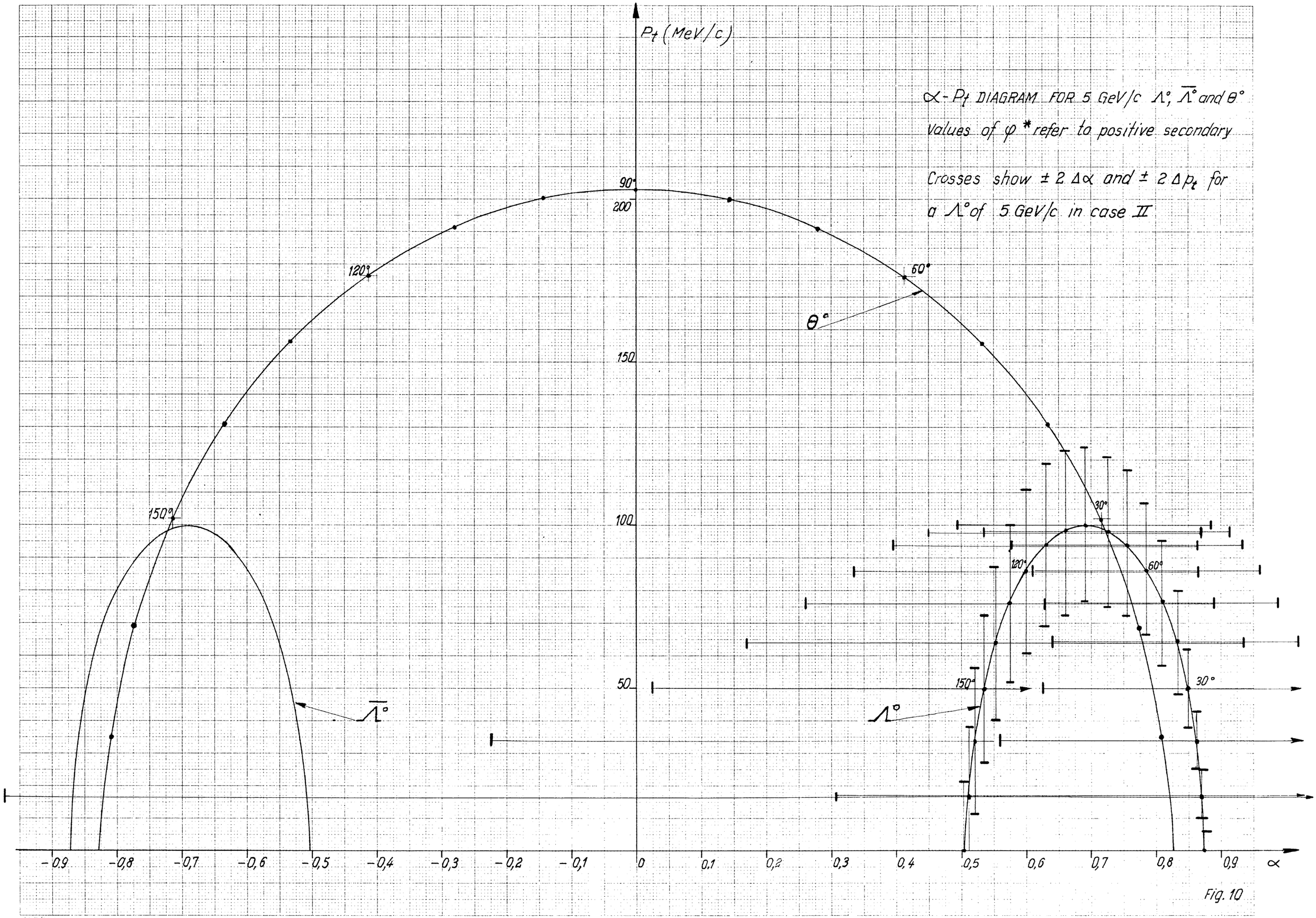

Fig. 10

$\alpha - P_t$ DIAGRAM FOR 5 GeV/c Λ°, $\bar{\Lambda}^\circ$ and θ°.
Values of φ^* refer to positive secondary
Crosses show $\pm 2\,\Delta\alpha$ and $\pm 2\,\Delta P_t$
for a θ° of 5 GeV/c in case II

P_t (MeV/c)

200
150
100
50

90°
120°
150°
60°
30°

$\bar{\Lambda}^\circ$
Λ°
θ°

−0,9 −0,8 −0,7 −0,6 −0,5 −0,4 −0,3 −0,2 −0,1 0 0,1 0,2 0,3 0,4 0,5 0,6 0,7 0,8 0,9 α

Fig. 11

SIS. R/1440